Colloids and Surfaces A: Physicochem. Eng. Aspects 500 (2016) 79–87

Contents lists available at ScienceDirect

Colloids and Surfaces A: Physicochemical and Engineering Aspects

journal homepage: www.elsevier.com/locate/colsurfa

Surface functionalization of silica particles for their efficient fluorescence and stereo selective modification

Laura C. Mugica[a], Braulio Rodríguez-Molina[a], Salvador Ramos[b], Anna Kozina[a,*]

[a] Instituto de Química, Universidad Nacional Autónoma de México, México, D.F., Mexico
[b] Instituto de Física, Universidad Nacional Autónoma de México, México, D.F., Mexico

HIGHLIGHTS

- Good silica particles APTES modification is obtained by adjusting solvent polarity.
- Coupling time between RBITC and particle amino groups is extremely important.
- RBITC is stable for a few days but may tear off the particle at long reaction times.

GRAPHICAL ABSTRACT

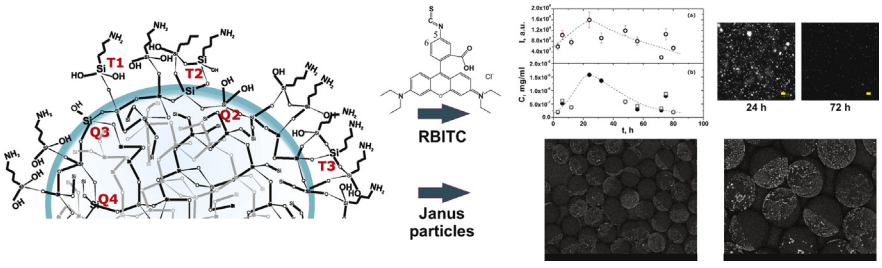

ARTICLE INFO

Article history:
Received 15 December 2015
Received in revised form 31 March 2016
Accepted 1 April 2016
Available online 2 April 2016

Keywords:
Silica particles
Surface modification
Fluorescence
Rhodamine B isothiocyanate
Janus particles

ABSTRACT

Optimization of reaction conditions between surface silanols of silica particles and 3-aminopropyltriethoxysilane is performed. A reasonably good surface coverage by amino groups is achieved by adjustment of solvent polarity, temperature and reaction time. The best results are obtained for the ratio of toluene/ethanol 9:1 (v/v) and 5 h of reaction time at 50 °C, which can be further improved increasing the surface amine density from 0.62 to 0.87 groups/nm^2 under dry silanization conditions. The availability of surface amino groups for further coupling is verified by decoration of anisotropically modified (Janus) particles with gold nanoparticles and by reaction with a fluorescent dye Rhodamine B isothiocyanate. The duration of coupling with the dye is crucial for efficient dye incorporation and particle fluorescence. The emission intensity of the dyed particles declines if the reaction is conducted for more than 24 h because of the degradation of the particle-dye adduct.

1. Introduction

Colloidal silica is widely used in a large number of areas such as ceramics and paper production, catalysis, electronics, metallurgy, optics, food and personal care products and chromatography [1]. Besides the creation of functional materials, in basic research nearly monodisperse silica particles serve as models for atomic and molecular systems, since their size allows their study by optical methods. Different phenomena of condensed matter physics such as crystallization, aggregation, glass transition as well as the connection between micro and macroscopic properties have been significantly addressed with help of model colloids [2–7]. One of the advantages of silica particles is the possibility of their surface modification that provides the 'tuning' of inter-particle interactions via surface coating with desirable functional groups. The coating may be homogeneous or patterned resulting in isotropic or anisotropic interactions, respectively [8].

Some of the functional groups widely used to cover silica are the amino groups, since they permit further particle conjugation with a chemical or biological entity. To coat the silica surface with amino groups, amino silanes are usually used as coupling agents, among which 3-aminopropyltriethoxysilane (APTES) is the most

* Corresponding author.
E-mail address: akozina@unam.mx (A. Kozina).

http://dx.doi.org/10.1016/j.colsurfa.2016.04.002
0927-7757/

commonly used due to wider exploration of its reaction with silica and its lower cost. Although the APTES-silica reaction seems straightforward, the resulting surface coverage is extremely sensitive to the synthesis conditions such as the silane concentration, reaction time, temperature, solvent polarity, and amount of water present. As it was shown previously, only a certain percent of surface silanols can be coupled to silanes and only a certain number of amino groups is available for further reactions [9]. Basically, the increase of reaction time and temperature leads to better surface coverage as well as the usage of apolar anhydrous solvents [10–13]. Nevertheless, a small amount of water is necessary to start silane hydrolysis, although the water excess may result in a poor surface modification because of the silane self-condensation in the reaction volume [14]. One difficulty to conduct the reaction in apolar solvents is that bare silica is highly hydrophilic and the particles cannot be well dispersed in a hydrophobic solvent. Another drawback to use apolar solvents is the synthesis of patterned particles, for example Janus particles in the simplest case [15]. Many times the synthesis includes the protection of a certain particle part while modifying the unprotected one [16,17]. However, the protection material may be apolar (e. g. wax) and, therefore, easily soluble in an affine solvent loosing its function of particle protection. Thus, the usage of an apolar solvent or high temperature is desirable but limited or inappropriate in some cases. These limitations put a demand to look for mild but efficient synthesis conditions that would still provide the desirable surface modification.

The reaction of conjugation of amino groups with fluorescent dyes have maintained an increased interest because it is commonly used to label proteins, antibodies and DNA for studies of their transport, specific interactions or folding as well as for fluorescent detection and imaging of certain constituents of living cells [18]. In the case of colloidal particles, optical fluorescent or confocal microscopy techniques demand labeling of particles with fluorescent dyes. Among many dyes, isothiocyanate derivatives of xanthene dyes such as Fluorescein (FITC) and Rhodamine B isothiocyanates (RBITC) are widely used. Although the quantum yield of RBITC is lower than that for FITC in aqueous solutions at neutral pH [19,20], the main advantage of RBITC is its better stability to photobleaching [18,21]. Another advantage is that the isothiocyanate dye derivatives covalently attach to primary amino groups forming relatively stable substrate-dye complexes. The resulting particle fluorescence increases as more RBITC molecules are attached to the surface up to a certain level. Over-labeling leads to a fluorescence quenching due to interactions between the dye molecules [22]. The reaction is usually carried out in the dark and under inert atmosphere to avoid fluorochrome decomposition. Although there are many suggestions for particle labeling protocol, there is still a lack of agreement for application of certain reaction conditions such as the reaction time, temperature or dye concentration. Moreover, it was mentioned previously that the reaction between APTES amino groups and RBITC is not complete even in excess of APTES [23]. The increase of the reaction time might help to improve the reaction efficiency and resulting particle fluorescence. Nevertheless, we are not aware of any studies of optimization of RBITC incorporation as a function of reaction time. Thus, we performed these experiments.

In the present work we optimized two steps in the surface modification of silica particles. We report the best conditions to achieve a significant surface coverage with amino groups using APTES. We show how this improved coverage helps to visualize selectively modified Janus particles by stereo selective attachment of affine gold nanoparticles. After optimization of particle reaction time with fluorescent dye RBITC we demonstrate that one can obtain the most intensive emission only in a certain reaction time interval.

2. Experimental

2.1. Materials

Silica particles with diameters of 320 nm, 500 nm, 1 and 3 μm and polydispersity indices of about 3% were used. The small and medium-size particles were synthesized by modified method of Stöber [24]. The largest particles were purchased from Bangs Laboratories (Fishers, USA), 3-aminopropyltriethoxysilane (APTES), Rhodamine B isothiocyanate (RBITC), didodecyldimethylammonium bromide (DDAB), paraffin wax, dichlorodimethylsilane (DCDMS), gold hydrochloride, sodium citrate, ethanol and toluene were purchased from Sigma–Aldrich (St. Louis, USA) and used as received. Glacial acetic acid and methanol were purchased from J. T. Baker Chemicals (Center Valley, USA). All the used water was purified according to HPLC standards.

2.2. Surface modification

Before the modification silica particles were cleaned with chromic acid and then surface activated by piranha solution (H_2SO_4/H_2O_2 7:3, v/v). The silanization with APTES was carried out in the four ways summarized in Table 1. For each sample a certain amount (adjusted to have equal total surface area) of clean silica particles was reacted with a certain amount of APTES in a given solvent. The synthesis conditions from Ref. [25] were chosen as the reference, since it was reported to result in a good surface coverage. Thus, the reaction temperature and time were kept at 50 °C and 5 h for all the samples except SA3, where they were changed to 25 °C and 24 h as explained later. After reaction time was complete, the particles were washed with the corresponding reaction solvent at least 5 times by sedimentation-redispersion procedure. To reproduce the reaction conditions from Ref. [25], the washings with toluene were followed by rinsing with the mixture of glacial acetic acid and methanol. For SA4 sample modification the mixture of toluene/ethanol was prepared as 9:1 by volume. In the case of dry reaction conditions, the sample was thermally pretreated at 140 °C for 2 h. Ethanol was dried by addition of KOH in reflux overnight followed by distillation under nitrogen atmosphere. Toluene was dried with sodium and left in reflux until the indicator (benzophenone) changed color to blue.

The synthesis of Janus particles followed the recipes from Refs. [26,27]. To be specific, 50 mg of the particles with diameter of 500 nm and 3 μm were cleaned as mentioned above for silanization and dispersed in 15 ml (for d = 500 nm) or 5 ml (for d = 3 μm) of the aqueous solution of DDAB with C = 0.044 and C = 0.011 g/l, respectively. The DDAB concentration was chosen so that the particles were to immerse at about a half of their volume. This dispersion was added to 1.5 or 0.5 g of molten paraffin wax at 75 °C and stirred for 20 min with a magnetic stirring bar to form a stable wax-in-water

Table 1
Conditions for particle silanization with APTES (particle diameter 320 nm). Here m_P is the weight of particles, m_S is the weight of APTES, m_S/A_P is the weight of APTES per sample area, T is the temperature and t_r is the reaction time.

Sample	m_P, mg	m_S, g	m_S/A_P, mg/nm^2	Solvent	T, °C	t_r, h
*SA*1	150	0.600	0.44	Toluene	50	5
*SA*2	150	0.600	0.44	Ethanol	50	5
*SA*3	200	0.097	0.10	Ethanol	25	24
*SA*4	150	0.600	0.39	Toluene/ethanol	50	5

emulsion. Then, the droplets were cooled to form solid colloidosomes and washed with deionized water to remove DDAB and unattached particles. The exposed particle surface was silanized with DCDMS in vapor according to Ref. [26] for 10 min, then the wax was dissolved in chloroform and the other particle side was modified by attaching APTES under the best previously established conditions.

Gold nanoparticles with diameter of 30 nm were synthesized by a standard method [28] using equal volumes and concentrations of aqueous solutions of gold hydrochloride as a precursor and sodium citrate as a reducing agent. First, the gold hydrochloride solution was heated until started to boil and then preheated citrate solution was added at vigorous stirring. The heating and stirring was kept until the reaction mixture was mauve colored and had not changed color during 5 min.

To attach the fluorescent dye RBITC, 100 mg of the APTES modified particles ($d = 1\ \mu m$) were reacted with 5 mg of RBITC in 20 ml of ethanol. The samples were thermostatted at 25 °C under nitrogen atmosphere and completely covered with aluminum foil to avoid RBITC photo decomposition. The reactions were started at the same time and stopped after certain time intervals by separation of particles from the reaction mixture. Then, the particles were thoroughly washed with clean ethanol by sedimentation-redispersion cycles. To assure the complete dye removal, each supernatant was checked by fluorescence spectroscopy and the washings were stopped when no peak attributed to RBITC emission was observed (about 30 times).

2.3. Surface characterization

Solid-state ^{13}C and ^{29}Si nuclear magnetic resonance (NMR) spectra were obtained in natural abundance at frequencies of 75.4 and 59.5 MHz, respectively, on a Bruker ASX300 spectrometer using a 4 mm CPMAS probe. Magic-angle spinning was carried out at 8 kHz (^{13}C) and 5 kHz (^{29}Si) for the removal of spinning sidebands. ^{13}C CPMAS spectra were obtained with a 2 ms contact time and a recycle of 5 s. ^{29}Si spectra were acquired using single-pulse or cross-polarization MAS techniques with a 5 ms contact time and a recycle time of 18 s. A total of 11,200 (^{13}C) and 10,400 (^{29}Si) accumulations were obtained for each spectrum. All chemical shifts are reported in parts per million. Solution-state ^{1}H and ^{13}C NMR spectra of RBITC were recorded with a Bruker Advance spectrometer at 300 MHz (^{1}H) and 75.4 MHz (^{13}C) in EtOD-d_6 as a solvent.

The RBITC-labeled particles were imaged under the confocal laser-scanning microscope equipped with $\lambda = 555$ nm laser mounted on a Zeiss Axioscope A1 (Carl Zeiss, Germany). The maximum pinhole aperture (13.55 AU) was used. The excitation was performed with the laser and the emission was collected with a filter at $\lambda = 605 \pm 30$ nm. Oil immersion objectives (Fluar 40×/NA 1.30 and alpha Plan-apochromate 100×/NA 1.46) were used for all the samples prepared by dropping a well-dispersed particles in toluene/ethanol mixture (9:1, v/v) on a microscopy slide followed by covering it with a cover-slide and sealing. The imaging conditions were maintained equal for all the samples: exposure time was fixed to 15.49 s, frame size to 2048 × 2048 pixels, laser intensity to 2% and camera gain to 600. The images were saved in a 16-bit gray scale TIFF format and the intensity of the image area corresponding to each particle was analyzed in Image J software. At least 100 single particles (avoiding aggregates) were analyzed and their intensities were averaged to obtain good statistics. The experiment was repeated three times starting from the APTES particle modification to the image analysis. The reported results are the average of those, while the error bars represent the standard deviation from the average.

UV–vis absorption and fluorescence emission spectra were recorded with a Varian Cary Bio UV–vis and Cary Eclipse fluorescence spectrophotometers. First, the maximum of absorbance was identified at $\lambda = 550$ nm, which corresponds to the main RBITC band. Then, to record the emission spectra the dye was excited at $\lambda = 550$ nm. To estimate the dye concentration present on the particle surface, the procedure reported by Giesche et al. [29] was used. To record the dye spectra, 10 mg of dyed particles were dissolved in 5 ml of 1 M NaOH solution. The fluorescent specie left after the particle dissolution was measured by UV–vis and fluorescent spectroscopy. To estimate RBITC concentration the calibration curves in 1 M NaOH and 1 M NaOH with previously dissolved 10 mg of silica particles were obtained.

3. Results and discussion

3.1. Modification with APTES

The surface of clean bare silica particles is covered with hydroxyl groups bound to silicon atoms. There can be one (single or vicinal) or two (geminal) hydroxyl groups bound to one silicon atom. The bulk of the particle consists of Si—O—Si network. Fig. 1 shows different types of silicon atoms present at the surface or in the bulk of silica particles on APTES modification. Since APTES molecule has three ethoxy groups, it has three potential reaction sites with surface silanols. In order to confirm that the bare particles are clean and evaluate available silanols, first, ^{29}Si NMR spectrum was obtained for clean bare particles as shown in Fig. 2.

There are two main peaks in the spectrum of the bare particles. The peak at −112 ppm corresponds to Q4 type of silicon atom that is the bulk silica, the peak at −103 ppm is Q3 and the shoulder at −93 is Q2 silicon atoms bound to one or two hydroxyl groups, respectively. Since the peak intensities in the SPMAS NMR spectra are proportional to the amount of the present species, we can conclude that the majority of the silanols are single (vicinal) with a small fraction of geminal ones. APTES molecule has three sites that potentially can bind with the surface silanols. However, in the case of reduced amount of water, there is a certain probability that not all the ethoxy groups of APTES molecules are hydrolyzed. Thus, one can expect that there may be some residual non-hydrolyzed ethoxy groups found on the particle surface after silanization.

Although SPMAS NMR technique has an advantage to allow the quantitative analysis of signals, the main disadvantage is a rather long spectrum acquisition time resulting in its high cost. Cross polarization $^{1}H \rightarrow {}^{29}Si$ or $^{1}H \rightarrow {}^{13}C$ NMR (CPMAS) overcomes this disadvantage enhancing the sensitivity of low natural abundance nuclei (such as ^{29}Si and ^{13}C), however, the signals cannot be easily quantified. Thus, to intensify the signals, the CP MAS technique was used for comparison of different particle surface modifications. Fig. 3 shows ^{29}Si and ^{13}C CPMAS NMR spectra for the modified silica samples including the bare silica particles as the reference. It is worth to mention that the bare silica in Fig. 3 presents the same peaks in ^{29}Si as those in Fig. 2 and does not show any peaks in ^{13}C spectrum. This is an indication of a clean surface of our particles before modification. The intensity of Q3 peak is now larger than that of Q4 due to better polarization of $(SiO)_3$—Si—OH moiety as compared to SiO_4. It also applies for all the other studied samples. The first sample SA1 was modified in pure toluene according to Ref. [25]. In order to disperse the hydrophilic particles in toluene we used Triton X100. As it is seen from Fig. 3, we have not observed any peaks besides the ones of the bare silica in ^{29}Si spectrum. There are two peaks in the ^{13}C spectrum at 17 and 63 ppm that correspond to the carbon atoms of APTES ethoxy groups. The presence of these groups is the indication of a very poor APTES hydrolysis. Apparently, the water adsorbed to the particle surface was not enough to start the silane hydrolysis, which resulted in a scant chemical modification. Most probably, the silane is just physically adsorbed

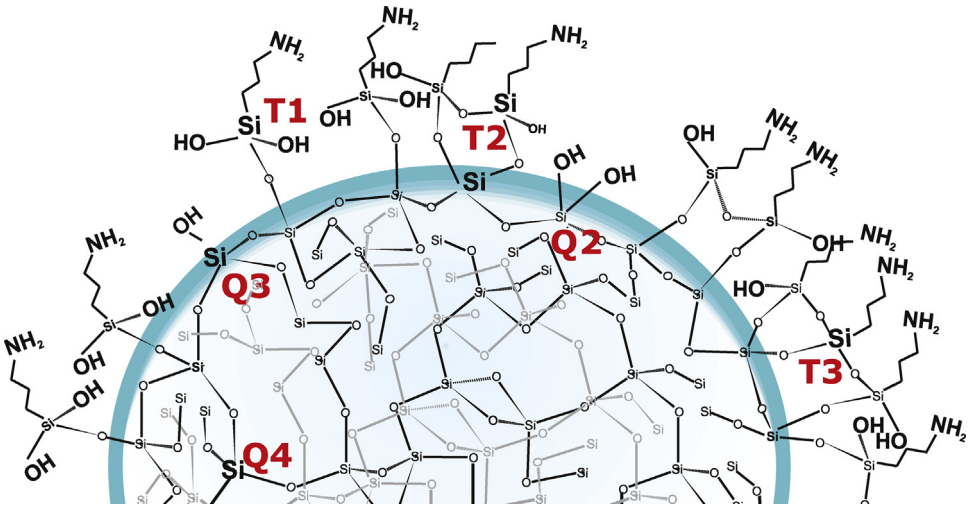

Fig. 1. Schematic representation of different types of silicon atoms bound to one, two or non of the surface hydroxyl groups (Q) and bonding types of APTES molecules to the particle surface (T).

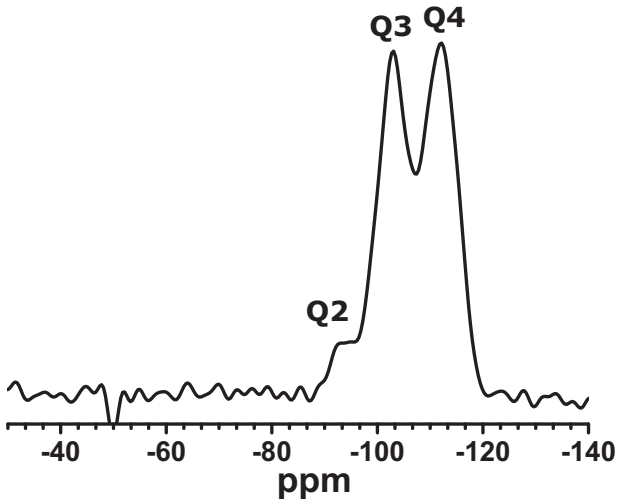

Fig. 2. ^{29}Si SPMAS spectrum of clean bare silica particles. Peaks at −112, −103 and −93 ppm correspond to Q4, Q3 and Q2 silicon atoms, respectively.

on the silica surface interacting with hydroxyl groups via hydrogen bonds. This interaction together with signals from methanol used for particle washing is also reflected in the small peak at 52 ppm [30]. There are some indications of the appearance of the peaks corresponding to C1–C3 atoms of APTES, however, they are too close to noise to draw any solid conclusion. Another observation that we made during the synthesis is that the particles, because of their high hydrophilicity, could not be dispersed completely in toluene even after addition of a good amount of Triton X100. Thus, even if all APTES was hydrolysed, it would be extremely difficult to obtain a homogeneous surface modification because of rather severe particle aggregation. Moreover, even after several washing cycles, there was still a small amount of the surfactant left on the particle surface, which is reflected in a small peak at 72 ppm. Thus, we can conclude that this method did not work well for our particles.

To avoid particle aggregation, it was decided to change the solvent to a more polar one. For this reason ethanol was used for the sample SA2 keeping the rest of the synthesis conditions the same as for SA1. However, the resulted modification was even worse than SA1 because ^{13}C CPMAS spectrum showed only the peaks corresponding to carbons of ethoxy groups. These peaks result from ethanol chemically or physically adsorbed to the particle surface

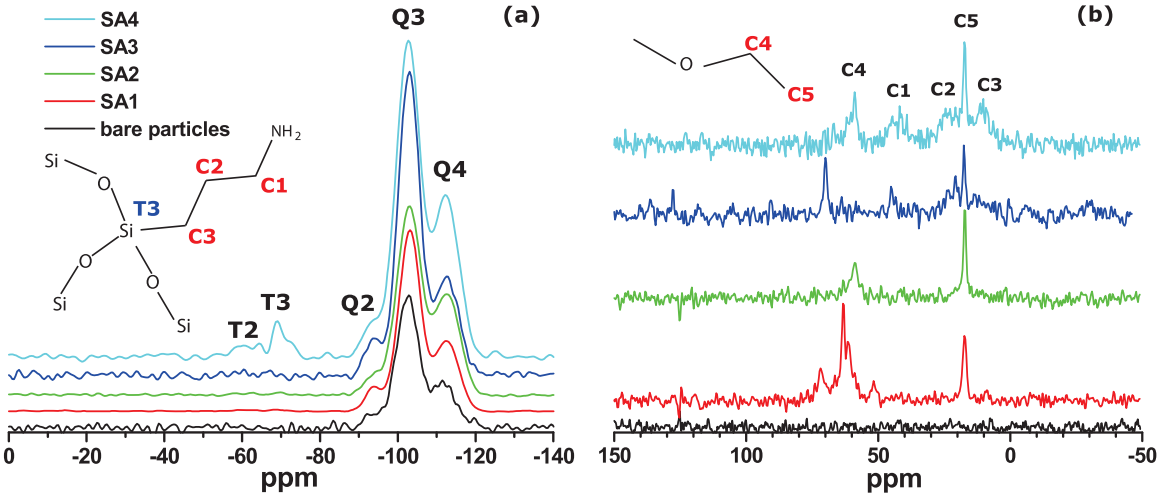

Fig. 3. CPMAS spectra of silica particles modified under different conditions, (a) ^{29}Si and (b) ^{13}C. The peak assignment follows Fig. 1. The inset in (a) shows APTES structure bound to silica surface, the inset in (b) represents carbon atoms assignment in ethoxy groups.

[30]. Although ethanol is a good solvent for APTES, it is known that the rate of the silane hydrolysis is accelerated in ethanol as compared to toluene. The faster hydrolysis also promotes APTES self-condensation in the bulk reducing its content at the surface. Another reason for poor modification is the ability of ethanol to interact strongly with the hydroxyl groups of the silica surface screening the APTES-silica interactions and hindering their surface condensation [10,30].

In order to slow down the APTES bulk polycondensation we decreased its amount per particle as well as the synthesis temperature (from 50 to 25 °C, sample SA3). To compensate for the expected decrease of the surface modification, we increased the reaction time from 5 to 24 h. The ^{13}C NMR spectrum in Fig. 3b shows that the modification was improved as compared with the previously in-ethanol modified sample SA2. Besides the two peaks of ethoxy species, the small peaks corresponding to C1–C3 APTES carbons appear at 10, 20 and 42 ppm. However, ^{29}Si spectrum does not present any peaks other than those of the bare silica. This fact together with the small peaks in the ^{13}C spectrum allow us to conclude that the modification of the particles proceeded well but the amount of the surface APTES is rather low. Nevertheless, these conditions may be useful in some cases when it is not possible to use an apolar solvent, for example, in the modification of the particles immersed in wax, including with or without stirring [31].

To combine the advantages that are provided by both polar and apolar solvents, sample SA4 was modified under the same conditions as SA1 and SA2 but in the mixture of toluene/ethanol (9:1, v/v). As it can be seen from Fig. 3b, the ^{13}C spectrum presents all the peaks corresponding to APTES and they are pronounced. The ethoxy species are still present, which may be the result of the exchange reaction between silica hydroxyls and ethanol or incomplete APTES hydrolysis because of lack of water. Despite the presence of ethoxy groups, the ^{29}Si spectrum also confirms the efficient modification with a new peak at −69 ppm and a barely appreciable peak at −60 ppm corresponding to T3 and T2 silicon atoms, respectively [33]. There are various reasons for the successful APTES reaction with silica in SA4 case. First, since the majority of the solvent is apolar, the hydrolysis of APTES is slowed down and its polycondensation in bulk is hindered. This allows the major part of the silane to be located close to the surface of silica, where the concentration of ethanol is the highest (ethanol has more affinity to hydroxyl groups than to toluene molecules). This increases the probability that APTES molecules attach to the particle surface. Second, high temperature improves the mobility of the surface ethanol layer as well as the APTES molecules, therefore, giving better opportunity to the silane to react with the surface. Finally, a small amount of ethanol helps significantly to disperse the bare, extremely hydrophilic silica particles improving the availability of the whole particle surface for modification.

It is known that the presence of water in the reaction mixture often leads to the formation of multilayers of APTES, where the molecules in the second and higher order layers interact via hydrogen bonds with the first layer. Thus, we performed additional experiments to eliminate water influence as well as the possibility of multilayer formation. First, we dried the particles prior the reaction by heating them for 2 h at 140 °C and used dry ethanol and toluene to prepare the solvent reaction mixture. Second, the total amount of amino groups was characterized by the method of Ritter et al. [32] (6.6 mg of d = 320 nm particles were dissolved). The calibration curve for fluorescamine and the corresponding sample spectra are shown in the supporting info. The calculated amount of the amino groups is 987.5 and 1399.3 nmol/m^2 for non-dry and dry conditions, respectively, which corresponds to 0.62 and 0.87 APTES molecules per nm^2 of silica surface. If we consider that one APTES molecule occupies maximum 3 hydroxyl groups of the silica surface, theoretically, the maximum surface coverage would yield 1.25–2.0 APTES molecules/nm^2 (taking into account the OH-group surface density of 4–6 OH/nm^2). The comparison of the experimental values with the estimated maximum eliminates the possibility of multilayer formation. The higher APTES load in the case of dry reaction conditions may be caused by the self-catalysis of APTES molecules. APTES amino groups can be either hydrogen bound or protonated by acidic silanols at the silica surface [33]. However, the condensation of the silane with the surface may occur with the further covalent bond formation. Such a process is known as flip-mechanism [34,35]. In the presence of adsorbed water at silica surface, this mechanism is hindered, while at the dry surface it is more favorable. Therefore, the measured surface coverage is higher after the dry synthesis conditions, although one disadvantage of such synthesis is its laboriousness and cost. One should mention that the amino group loading obtained in the present work compares very well with the one previously reported [32] but for vapor APTES deposition. It is worth to say that the vapor deposition method cannot be applied for our particles, since it will result in a non-homogeneous surface coverage because of particle aggregation. Thus, our method has an obvious advantage, since it provides the comparable amino group coverage in solution. The 100% coverage is hardly possible as discussed earlier [35]. The problem is that only some APTES amino groups that form hydrogen bonds with the surface silanols may self-catalyze the condensation with the further covalent bond formation. However, another fraction of molecules (about 32%) does not flip and stays only physically adsorbed to the surface. These molecules are easily detached from the surface on washing resulting in only about 68% of covalently bound amines [34,35]. Taking into account this fact, our surface modification may be considered as successful, since we obtain 49.6 and 69.6% of the total amino group coverage in the case of non-dry and dry silanization conditions, respectively.

3.2. Synthesis of Janus particles

To further explore the success of the amino group attachment, anisotropically modified Janus particles were synthesized. The silanization with APTES was performed under the same conditions as for SA4 sample. As it is well-known, citrate-stabilized gold nanoparticles have affinity to amino groups because of the strong electrostatic interactions between negatively charged carboxyl and positively charged amino groups in water. Thus, the attachment of gold nanoparticles to silica surface can help to visualize the part of the surface covered with amino groups. Thus, gold nanoparticles were attached selectively to amino modified particle surface. Fig. 4 shows the SEM images of Janus silica particles regio-selectively decorated by gold nanoparticles. As it is seen from the images, only one side of the particles is covered with gold. This indicates that the whole procedure of the Janus synthesis works well and the silanization with APTES is very successful independently from the particle size. The density of the attached gold NPs is rather high, which allows us to conclude that the density of the attached amino groups is also sufficient to assure any further conjugation.

3.3. RBITC labeling

In order to explore further the availability of the amino groups, their coupling with RBITC was studied as a function of the reaction time. Before the reaction with the dye, particles with diameter of 1 μm were modified in the same way as sample SA4 keeping APTES/particle area ratio equal to 0.44 mg/nm^2. Fig. 5 shows the fluorescence of the resulting particles as seen by optical microscopy and UV–vis and fluorescence spectroscopy. The particle optical micrographs and UV–vis absorption and fluorescence spectra may be found in supporting info. The fluorescence intensity as seen by

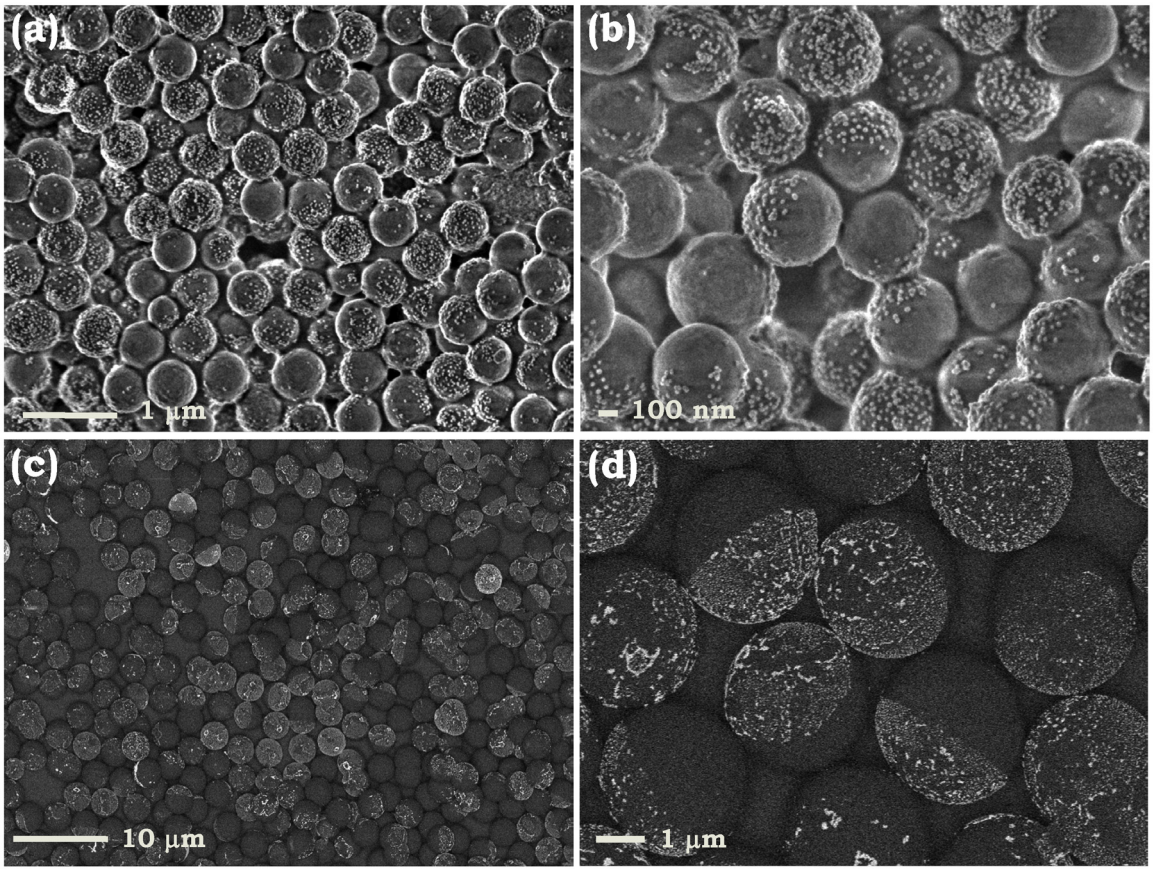

Fig. 4. Scanning electron microscopy images of silica particles selectively decorated by gold nanoparticles. (a) and (b) correspond to 500 nm and (c) and (d) correspond to 3 μm Janus particles. The decorated parts indicate successful selective surface modification with amino groups.

optical microscopy (Fig. 5a) first increases with reaction time up to 24 h and then gradually decreases with a small peak at 75 h. This tendency is remarkable and unexpected because one would think that the increase of the reaction time should result in the attachment of more molecules of RBITC to the particle surface and, as a result, in stronger fluorescence. There are two possible reasons that may explain the opposite effect that we observe: (i) the dye fluorescence quenches because there are too many molecules attached to the surface and (ii) the dye surface concentration decreases with long reaction time and so does its fluorescence. To check these ideas we dissolved 10 mg of each sample in 1 M solution of NaOH and measured the concentration of the remained specie, which in this case would be RBITC attached to the modified APTES, which probably will have the hydroxyl group instead of the silicon atom. The extinction coefficient of RBITC in 1 M NaOH is found to be 5.9×10^6 $(M\,m)^{-1}$. To check that the formation of Na_2SiO_3 does not modify the RBITC solubility and fluorescence, the calibration curve of the dye in 1 M NaOH previously reacted with 2 mg/ml dispersion of silica particles was also measured. The extinction coefficient in this case is found to be 6.3×10^6 $(M\,m)^{-1}$, rather close to that in a pure sodium hydroxide solution. The two emission calibration curves are very close to each other (see supporting info). Fig. 5b shows that both UV–vis absorption and fluorescence emission measurements are in a very good agreement in estimation of the dye concentration (the fluorescence signal was saturated for 24 and 32 h). The concentration follows well the tendency obtained by miscroscopy, it increases up to 24 h and then gradually decreases. These results eliminate the possibility of the fluorescence quenching due to high dye surface concentration. Also, the calculation of the amount of attached RBITC yields 846 molecules/particle or about 3×10^{-4} molecules/nm^2, so that the dye molecules are rather separated and it is unlikely that they quench each other fluorescence. The only possible explanation for such a decrease in fluorescence is a drop of the dye concentration on the particle surface with time. To explore this possibility let us first look at Fig. 6 that shows the structure of RBITC molecule.

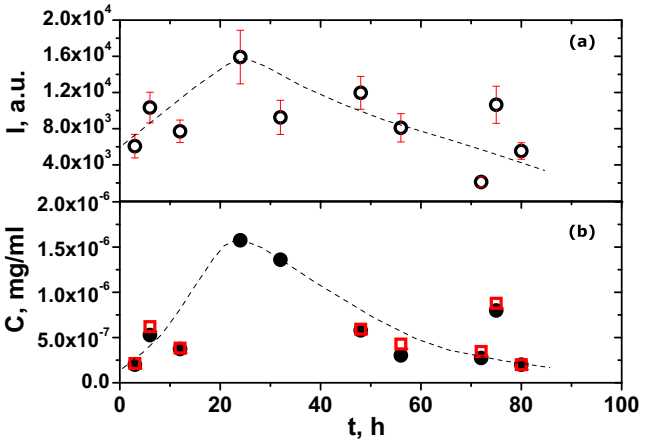

Fig. 5. (a) Fluorescence intensity of the particles as seen by optical microscopy as a function of reaction time with RBITC. (b) Concentration of RBITC in 5 ml of 1 M NaOH after dissolution of 10 mg of particles calculated from UV–vis (filled circles) and fluorescence (open squares) spectroscopy. Thin dashed lines are guides for the eye.

Strong absorption and fluorescence in the visible wavelength range is due to xanthene ring conjugation. Therefore, a significant decrease of absorption and fluorescence signals may result from

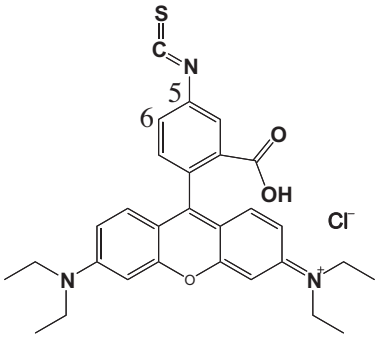

Fig. 6. Rhodamine B isothiocyanate, NCS-group may be located in position 5 or 6 of the benzene ring forming the mixture of isomers.

two possible reasons: (i) the fluorophore is degraded with time in such a way that the conjugation of xanthene ring is lost and (ii) the molecule is intact in the xanthene ring but it detaches from the particle surface with time and is eliminated on particle washing.

It is known that many fluorophores tend to decompose under certain conditions such as extreme pH and temperatures, light and oxygen exposure, etc. Thus, we first measured the RBITC stability in pure ethanol, in 1 M solution of NaOH and in ethanol with addition of a small amount of 1 M aqueous solution of hydrochloric acid. Fig. 7 shows the spectra for only one selected concentration of the dye, although three concentrations were actually measured and showed no difference in the tendency. The spectra have the main absorption band at 540 nm in ethanol and 550 nm under basic or acid conditions. The small shift in the main peak position is normal on the change of medium polarity, which indicates changes in electron transitions. What is impressive is that the peaks are completely reproduced with time and no other bands appear. Therefore, the fluorophore is very stable in all the mentioned mediums at least up to 1 week.

To further confirm xanthene structure stability, NMR spectra in deuterated ethanol-d_6 were also recorded. Besides the freshly prepared dye, RBITC that was in the reaction mixture with the particles for 75 h was also measured. Fig. 8 shows the corresponding spectra. To monitor a possible change of the main species concentration, pyrene was used as an internal standard inside a capillary in all the experiments except the one for 75 h. The peaks of the reference appear between 7.7 and 8.0 ppm interfering with the signals from the benzene ring of RBITC. The signals from the hydrogens of xanthene ring appear between 6.5 and 7.5 ppm, while aliphatic

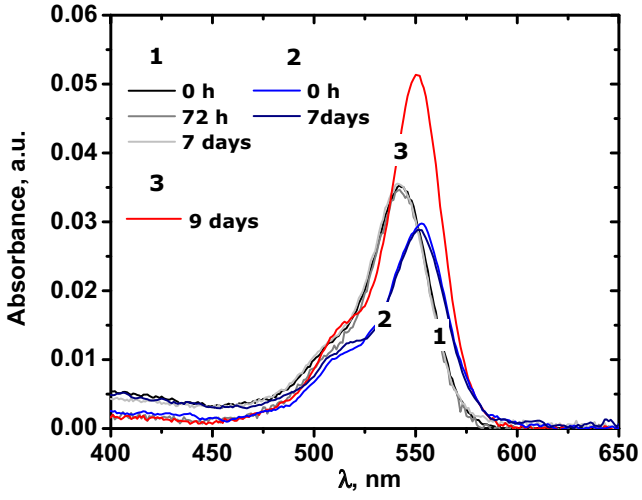

Fig. 7. UV–vis absorption spectra of RBITC at $C = 5 \times 10^{-4}$ mM as a function of time in (1) ethanol, (2) 1 M solution of NaOH and (3) ethanol/HCl 500/1, v/v.

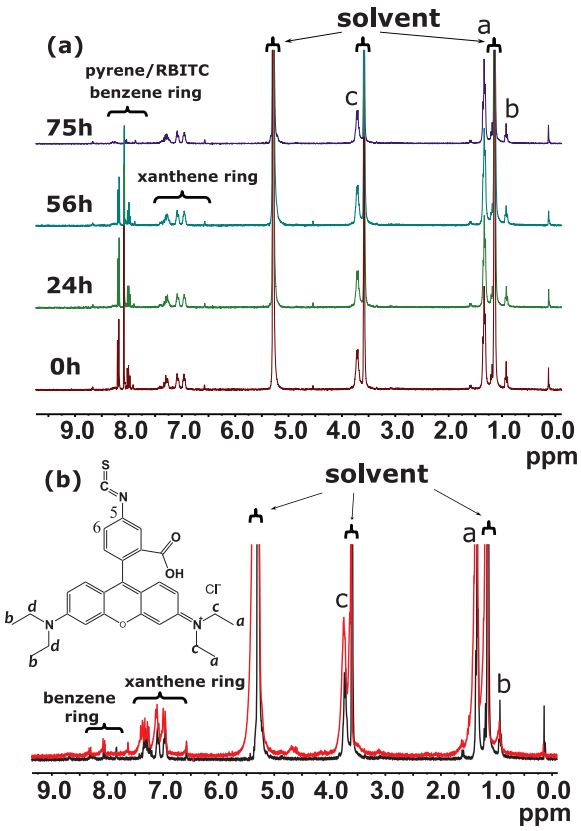

Fig. 8. ^{1}H NMR spectra of RBITC in EtOD-d_6: (a) time evolution of freshly prepared RBITC and (b) comparison of RBITC after 75 h of evolution without particles (black) and in the presence of particles (red). (For interpretation of the references to color in this figure legend, the reader is referred to the web version of the article.)

hydrogens contribute to the peaks *a*, *b* and *c* below 4 ppm as labeled in the inset of Fig. 8b. As it is clearly seen from the time evolution, the structure of the dye is intact up to 75 h in ethanol. The comparison of the intensities of the signals from the sample and the standard resulted in the same proportion for all the waiting times indicating constant dye concentration. Apparently, the contact with the particles also does not affect the RBITC structure as it is seen from Fig. 8b. The region of the signals corresponding to xanthene ring is not affected, which implies that the ring conjugation and as a result its UV–vis absorption and fluorescence should be intact. We also recorded ^{13}C NMR spectra of the dye (see supporting info), however, it was not possible to obtain very intense signals even after a few days of measuring because of the low solubility (about 5 mg/ml) of RBITC in ethanol. Nevertheless, there is a small indication that after the contact with particles a small part of the dye converts to N,N,N′-triethylrhodamine, where one ethyl group (*b* and *d* atoms) is eliminated. It is known that this may happen with RBITC during the oxidation process as a result of light and oxygen exposure [36,37]. Such a N-dealkylation should result in a 10 nm hypsochromic shift of the absorption maximum. We have not observed the mentioned change probably because only a small part of the dye was N-dealkylated and the overall absorption and fluorescence spectra were not affected.

The experiments on the RBITC stability allow us to conclude that the xanthene ring, the part responsible for absorption and fluorescence, does not degrade in time even in the presence of the particles. Therefore, the only possible reason for the loss of the fluorescence is that the dye starts to tear off the particles and is washed away during the particle washing, thus, the total dye concentration drops. The part of the dye that chemically reacts with the particles is the isothiocyanate group. It forms thiourea linkage with

the APTES amino group. There are some reports that the isothiocyanate group is not stable over time and the efficiency of the dye coupling decreases if an old dye solution is used [18]. For example, there are indications of the hydrolysis of the isothiocyanate group before the reaction, although, it was shown that its degree is not significant to compete with the amine conjugation [18,38]. What was shown to be important is the significant hydrolysis of the thiourea bond linkage between the dye and the amine substrate [38]. The authors showed that the dye-substrate bond rupture is not an immediate process but starts being significant after 48 h and it reaches its prominence by 75 h of the incubation of a dye-substrate in a buffer solution. Indeed, thiourea and its derivatives can be hydrolized in water, acidic or basic media mainly according to the following scheme [39–41]:

$$(NH_2)_2CS + 2H_2O \rightarrow 2NH_3 + CO_2 + H_2S. \quad (1)$$

Thus, the RBITC-APTES adduct also may suffer the hydrolysis reaction, which might result in the formation of the two amines: RB-NH_2 and amino-modified silica particles besides CO_2 and H_2S. Although, a closer look into this process is necessary to draw a valid conclusion about the exact final products. Taking into account the possibility of mentioned hydrolysis and excluding the other potential reasons, the present experiments allow us to conclude that the dye-particle conjugate is indeed deteriorated with time very likely because of the rupture of the thiourea linkage. Since the process is more pronounced after 24 h of reaction time, it is not recommended to exceed this reaction time for efficient particle labeling. Potentially, this should also apply to isothiocyanate derivatives of other dyes.

4. Conclusions

We showed that a good surface modification of silica particles may be achieved by optimization of the synthesis conditions and mainly by adjustment of the solvent polarity. The ratio of toluene/ethanol 9:1 by volume results in a significant coverage of the particle surface with amino groups. The availability of the amino groups for further reaction is confirmed by their conjugation with affine gold nanoparticles as well as with a fluorescent dye RBITC. The reaction time with the dye is shown to be crucial to obtain the best fluorescence intensity. After reaching a maximum at 24 h of reaction time, the particle fluorescence declines most probably because of the rupture of the dye-particle linkage.

Acknowledgements

Financial support from CONACyT (project 238618) and DGAPA-UNAM (IA100215) are gratefully acknowledged. We appreciate the technical assistance of Marco A. Vera-Ramírez, Elizabeth Huerta-Salazar and María de los Ángeles Peña-González with NMR spectroscopy measurements, and Carlos Magaña with SEM observations. We are thankful to Rolando Castillo and Jorge Peon Peralta for access to laboratory facilities.

Appendix A. Supplementary data

Supplementary data associated with this article can be found, in the online version, at http://dx.doi.org/10.1016/j.colsurfa.2016.04.002.

References

[1] H.E. Bergna, W.O. Roberts, Colloidal Silica: Fundamentals and Applications, CRC Press, 2005.
[2] P.N. Pusey, J.P. in Hansen, D. Levesque, J. Zinn-Justin, Liquids, Freezing and Glass Transition, North Holland, Amsterdam, 1991.
[3] N.A.M. Verhaegh, H.N.W. Lekkerkerker, in: F. Mallamace, H.E. Stanley (Eds.), The Physics of Complex Systems, International School of Physics "Enrico Fermi", Course CXXXIV, IOS Press, 1997.
[4] P.J. Lu, D.A. Weitz, Colloidal particles: crystals, glasses, and gels, Annu. Rev. Condens. Matter Phys. 4 (2013) 217–233.
[5] D.A. Weitz, B. in Duplantier, T.C. Halsey, V. Rivasseau, Glasses and Grains, Springer Basel AG, 2011.
[6] T. Palberg, Crystallization kinetics of colloidal model suspensions: recent achievements and new perspectives, J. Phys.: Condens. Matter 26 (2014) 333101.
[7] A. Kozina, P. Díaz-Leyva, C. Friedrich, E. Bartsch, Structural and dynamical evolution of colloid-polymer mixtures on crossing glass and gel transition as seen by optical microrheology and mechanical bulk rheology, Soft Matter 8 (2012) 1033–1046.
[8] J. Du, R.K. O'Reilly, Anisotropic particles with patchy, multicompartment and Janus architectures: preparation and application, Chem. Soc. Rev. 40 (2011) 2402–2416.
[9] Y. Nakahara, T. Takeuchi, S. Yokoyama, K. Kimura, Quantitative 1H NMR analysis of reacted silanol groups in silica nanoparticles chemically modified with monochlorosilanes, Surf. Interface Anal. 43 (2011) 809–815.
[10] I.J. Bruce, T. Sen, Surface modification of magnetic nanoparticles with alkoxysilanes and their application in magnetic bioseparations, Langmuir 21 (2005) 7029–7035.
[11] R.M. Pasternack, S.R. Amy, Y.J. Chabal, Attachment of 3-(aminopropyl) triethoxysilane on silicon, Langmuir 24 (2008) 12963–12971.
[12] E.T. Vandenberg, L. Bertilsson, B. Liedberg, K. Uvdal, R. Erlandsson, H. Elwing, I. Lundström, Structure of 3-aminopropyl triethoxy silane on silicon oxide, J. Colloid Interface Sci. 147 (1991) 103–118.
[13] J.A. Howarter, J.P. Youngblood, Optimization of silica silanization by 3-aminopropyltriethoxysilane, Langmuir 22 (2006) 11142–11147.
[14] N. Gartmann, C. Schütze, H. Ritter, D. Brühwiler, The effect of water on the functionalization of mesoporous silica with 3-aminopropyltriethoxysilane, J. Phys. Chem. Lett. 1 (2010) 379–382.
[15] A. Walther, A.H.E. Müller, Janus particles: synthesis, self-assembly, physical properties, and applications, Chem. Rev. 113 (2013) 5194–5261.
[16] A. Perro, S. Reculusa, S. Ravaine, E. Bourgeat-Lamic, E. Duguet, Design and synthesis of Janus micro- and nanoparticles, J. Mater. Chem. 15 (2005) 3745–3760.
[17] L. Hong, S. Jiang, S. Granick, Simple method to produce Janus colloidal particles in large quantity, Langmuir 22 (2006) 9495–9499.
[18] G.T. Hermanson, Bioconjugate Techniques, Academic Press, 2013.
[19] T. López Arbeloa, F. López Arbeloa, P. Hernandez Bartolomé, I. López Arbeloa, On the mechanism of radiationless deactivation of rhodamines, Chem. Phys. 160 (1992) 123–130.
[20] R. Sjöback, J. Nygren, M. Kubista, Absorption and fluorescence properties of fluorescein, Spectrochim. Acta A 51 (1995) L7–L21.
[21] R.F. Kubin, A.N. Fletcher, Fluorescence quantum yields of some rhodamine dyes, J. Lumin. 27 (1982) 455–462.
[22] F. López Arbeloa, P. Ruiz Ojeda, I. López Arbeloa, Fluorescence self-quenching of the molecular forms of rhodamine B in aqueous and ethanolic solutions, J. Lumin. 44 (1989) 105–112.
[23] N.A.M. Verhaegh, A. van Blaaderen, Dispersions of rhodamine-labeled silica spheres: synthesis, characterization, and fluorescence confocal scanning laser microscopy, Langmuir 10 (1994) 1427–1438.
[24] J.H. Zhang, P. Zhan, Z.L. Wang, W.Y. Zhang, N.B. Ming, Preparation of monodisperse silica particles with controllable size and shape, J. Mater. Res. 18 (2003) 649–653.
[25] T. Sen, I.J. Bruce, Surface engineering of nanoparticles in suspension for particle based bio-sensing, Sci. Rep. 2 (2012) 564–570.
[26] S. Jiang, M.J. Schultz, Q. Chen, J.S. Moore, S. Granick, Solvent-free synthesis of Janus colloidal particles, Langmuir 24 (2008) 10073–10077.
[27] A. Perro, F. Meunier, V. Schmitt, S. Ravaine, Production of large quantities of "Janus" nanoparticles using wax-in-water emulsions, Colloids Surf. A: Physicochem. Eng. Aspects 332 (2009) 57–62.
[28] G. Frens, Controlled nucleation for the regulation of the particle size in monodisperse gold suspensions, Nat. Phys. Sci. 241 (1973) 20–22.
[29] H. Giesche, E. Matijević, Well-defined pigments: I. Monodispersed silica-acid dyes systems, Dyes Pigments 17 (1991) 323–340.
[30] M. Szekeres, O. Kamalin, P.G. Grobet, R.A. Schoonheydt, K. Wostyn, K. Clays, A. Persoons, I. Dékány, Two-dimensional ordering of Stöber silica particles at the air/water interface, Colloids Surf. A: Physicochem. Eng. Aspects 227 (2003) 77–83.
[31] S. Jiang, Q. Chen, M. Tripathy, E. Luijten, K.S. Schweizer, S. Granick, Janus particle synthesis and assembly, Adv. Mater. 22 (2010) 1060–1071.
[32] H. Ritter, M. Nieminen, M. Karppinen, D. Brühwiler, A comparative study of the functionalization of mesoporous silica MCM-41 by deposition of 3-aminopropyltrimethoxysilane from toluene and from the vapor phase, Microporous Mesoporous Mater. 121 (2009) 79–83.
[33] G.S. Caravajal, D.E. Leyden, G.R. Quinting, G.E. Maciel, Structural characterization of (3-aminopropyl)triethoxysilane-modified silicas by silicon-29 and carbon-13 nuclear magnetic resonance, Anal. Chem. 60 (1988) 1776–1786.
[34] K.C. Vrancken, P. van der Voort, K. Possemiers, E.F. Vansant, Surface and structural properties of silica gel in the modification with γ-aminopropyltriethoxysilane, J. Colloid Interface Sci. 174 (1995) 86–91.
[35] N.R.E.N. Impens, P. van der Voort, E.F. Vansant, Silylation of micro-, meso- and non-porous oxides: a review, Microporous Mesoporous Mater. 28 (1999) 217–232.

[36] T. Watanabe, T. Takirawa, K. Honda, Photocatalysis through excitation of adsorbates. 1. Highly efficient N-deethylation of rhodamine B adsorbed to CdS, J. Phys. Chem. 81 (1977) 1845–1851.
[37] T. Wu, G. Liu, J. Zhao, Photoassisted degradation of dye pollutants. V. Self-photosensitized oxidative transformation of rhodamine B under visible light irradiation in aqueous TiO_2 dispersions, J. Phys. Chem. 102 (1998) 5845–5851.
[38] P.R. Banks, D.M. Paquette, Comparison of three common amine reactive fluorescent probes used for conjugation to biomolecules by capillary zone electrophoresis, Bioconj. Chem. 6 (1995) 447–458.
[39] W.R. Shaw, D.G. Walker, Kinetic studies of thiourea derivatives. IV. The methylated thioureas. Conclusions, J. Am. Chem. Soc. 80 (1958) 5337–5342.
[40] E.A. Shitikova, T.P. Dyachkova, The Effects of Calurea and Thiourea on the Corrosion of Carbon Steel in Acid Chloride Media. Problems of Contemporary Science and Practice, vol. 3, Vernadsky University, 2006, pp. 209–216.
[41] T.V. Vinogradova, V.F. Markov, L.N. Maskaeva, Temperature dependence of constants of thiourea hydrolytic decomposition and cyanamide. Stepwise ionization, Russ. J. Gen. Chem. 80 (2010) 2341–2346.